NREL
NATIONAL RENEWABLE ENERGY LABORATORY

A RANS Simulation of the Heave Response of a Two-Body Floating Point Wave Absorber

Preprint

Y. Yu and Y. Li

To be presented at ISOPE 2011
Maui, Hawaii
June 19-24, 2011

Conference Paper
NREL/CP-5000-50980
March 2011

Contract No. DE-AC36-08GO28308

NOTICE

Available electronically at http://www.osti.gov/bridge

Available for a processing fee to U.S. Department of Energy
and its contractors, in paper, from:

U.S. Department of Energy
Office of Scientific and Technical Information

P.O. Box 62
Oak Ridge, TN 37831-0062
phone: 865.576.8401
fax: 865.576.5728
email: mailto:reports@adonis.osti.gov

Available for sale to the public, in paper, from:

U.S. Department of Commerce
National Technical Information Service
5285 Port Royal Road
Springfield, VA 22161
phone: 800.553.6847
fax: 703.605.6900
email: orders@ntis.fedworld.gov
online ordering: http://www.ntis.gov/help/ordermethods.aspx

Cover Photos: (left to right) PIX 16416, PIX 17423, PIX 16560, PIX 17613, PIX 17436, PIX 17721

Printed on paper containing at least 50% wastepaper, including 10% post consumer waste.

A RANS Simulation of the Heave Response of a Two-Body Floating-Point Wave Absorber

Yi-Hsiang Yu and Ye Li
National Wind Technology Center
National Renewable Energy Laboratory (NREL)
Golden, CO, 80401, USA

ABSTRACT
This paper presents a preliminary study on a two-body floating-point wave absorber. For this study, a Reynolds-Averaged Navier-Stokes (RANS) computational method was applied for analyzing the hydrodynamic heave response of the absorber in operational wave conditions. The two-body floating wave absorber contains a float section and a submerged reaction section. For validation purposes, the model was first assumed to be locked. The two sections were forced to move together as a single rigid body. The locked single-body model was used in a heave decay test that validated the RANS result with the experimental measurement. For the two-body floating-point absorber simulation, the two sections were connected through a mass-spring-damper system, which simulated the power takeoff mechanism under design wave conditions. Overall, the details of the flow around the absorber and its nonlinear interaction with waves were investigated. The power absorption efficiency of the two-body floating wave absorber in waves with a constant value spring-damper system was also examined.

KEYWORDS
Wave energy conversion (WEC); heave; Reynolds-averaged Navier-Stokes (RANS) equations; volume of fluid (VOF); free surface; floating-point absorber (FPA); power take-off (PTO)

INTRODUCTION
The extraction of energy from ocean waves has gained interest in recent years (Thorpe, 1999). A wide variety of technologies have been developed for converting wave energy into useful power, and many wave energy conversion (WEC) designs have been proposed. Falcão (2010) and Drew et al. (2009) recently reviewed the fundamental operating principles of the technologies that have been used for WEC devices. These include oscillating water columns, bottom-hinged pitch devices, floating pitch devices, overtopping devices, and floating-point absorbers (FPAs). The FPA is regarded as one of the simplest and most promising WEC systems and will be the focus of this paper.

The study of WEC can be traced back to 1970s. Researchers first investigated the potential for harnessing energy from waves by using potential flow methods. Their studies were focused on understanding the complex hydrodynamics of the FPA and on predicting the maximum wave power absorption. Specifically, the studies focused on the wave absorption width (Budal and Falnes, 1975; Evans, 1976; Mei, 1976) and on the wave power that can be absorbed by a given submerged body volume (Budal and Falnes, 1980). Reviews on these analytical works were presented in Falnes (2002; 2007). More recent research focuses on improving the wave absorption efficiency of the system. As demonstrated in an experimental analysis (Bjarte-Larsson and Falnes, 2006),the heave response and the converted power of an axisymmetric heaving WEC were significantly increased through the use of hydraulic power take-off (PTO) and latching control. Several additional studies focused on the optimal control strategy for waves (Korde, 1999; Yavuz et al., 2007), and an introduction to the fundamental theories for control and related tuning methods were described in Falnes (2002). However, these potential flow methods cannot provide accurate results because the nonlinear interaction between waves and the WEC device are assumed to be small, and the wave breaking and overtopping effects are excluded. A comprehensive understanding of a device requires the use of experimental methods or more advanced numerical methods such as the Reynolds-averaged Navier-Stokes (RANS) method. For example, Agamloh et al. (2008) used RANS to study the power capturing efficiency of cylinder type buoys with a PTO mechanism.

Typically, FPAs are either single-body or multiple-body devices. For the single-body FPA, Yeung (2010) presented a systematic study on both hydrodynamics and power electronic problems. This paper presents a study on a two-body FPA system. In general, a two-body FPA system includes a float section and a reaction section, and the system converts energy by utilizing the relative motion between the two sections. An example of a two-body FPA is Ocean Power Technology's (OPT's) Power Buoy. OPT deployed two 40-kW utility-scale systems, one in Santona, Spain in 2008 and the other in Ohau, Hawaii in 2009 (Fig. 1).

Figure 1. A prototype of OPT's PowerBuoy wave energy generation system. NREL PIX # 17114

The ability to design efficient PTO systems is critical for the success of the wave energy industry. In particular, it is essential to understand the complex hydrodynamics of FPA wave energy systems. Accordingly, the main objective of this research was to analyze the hydrodynamics of a two-body FPA system and its power output in operational wave climates. Only the heave motion was considered in this study. After presenting the numerical method and the numerical wave tank settings, a heave decay test was performed to validate the numerical model, where the floating section and the reaction section were assumed to be locked and moved as a single rigid body. The two sections of the FPA were connected through a mass-spring-damper system, which was applied to model the PTO mechanism. The details of the flow around the FPA model, the translating motion of the two sections, as well as their motion velocity, were examined. In addition, the maximum power that this particular two-body FPA model can absorb was studied.

MODELING

RANS method

A finite volume method-based RANS model (StarCCM+) was applied for solving the details of the unsteady incompressible flow field around the FPA under various wave conditions. The continuity equation and the Navier-Stokes equations are given as

$$\nabla \cdot \mathbf{U} = 0, \qquad \rho(\mathbf{U}_t + \mathbf{U} \cdot \nabla \mathbf{U}) = -\nabla p + \mathbf{F}_b + \nabla \cdot \mathbf{T} \tag{1}$$

where ρ is the water density, $\mathbf{U}$ is the flow velocity vector , and $\mathbf{U}_t$ is its time derivative, $\mathbf{F}_b$ is the body force vector (e.g., gravity), and $\mathbf{T}$ is the stress tensor.

The governing equations were discretized over a computational mesh and were solved using the transient SIMPLE algorithm to linearize the equations and to achieve pressure-velocity coupling. The resulting set of algebraic equations was solved through the use of an algebraic multigrid method. A k-ω SST turbulence model was applied with a two-layer all y+ wall treatment model, and a second order implicit scheme was applied for time marching. The water free surface was captured using a VOF method. The mesh around the FPA followed the FPA motion. A morphing model was adopted to move the mesh, and an arbitrary Lagrangian-Eulerian method was applied for handling the cell movement and its deformation.

In the study, the FPA only was allowed to move in heave, and the mooring system was not considered. The heave response was calculated by solving the equation of motion, which is given as

$$m_b a_t = F_d + F_{PTO} \tag{2}$$

where m_b is the mass of the body, a_t is the acceleration, and F_d is the dynamic force on the body, including the wave load, the buoyancy force, and the weight of the body. In addition to F_d, the PTO force F_{PTO} is the only external force acting on the system. The corresponding heave displacement was calculated by integrating the accelerations over time, and the equation of motion calculation was coupled with the RANS simulation through iterations.

Numerical wave tank settings

Figure 2 shows the computational domain and the domain boundaries of the numerical wave tank. To reduce the size of the problem, a symmetric boundary was applied along the x-z plane. The water depth was equal to 70m. The computational domain was 100m wide (0m≤y≤100m), 170m high (-70m≤z≤100m), and 7 wavelengths long (-2λ≤x≤5λ). The incident wave condition was specified at the inflow boundary. A sponge-layer method was applied, in which a damping zone (2λ in the wave propagation direction) was placed in front of the down wave boundary to absorb the outgoing and reflecting waves, without creating additional numerical disturbance. This sponge-layer method was tested successfully using the same numerical wave tank settings and without the presence of the absorber.

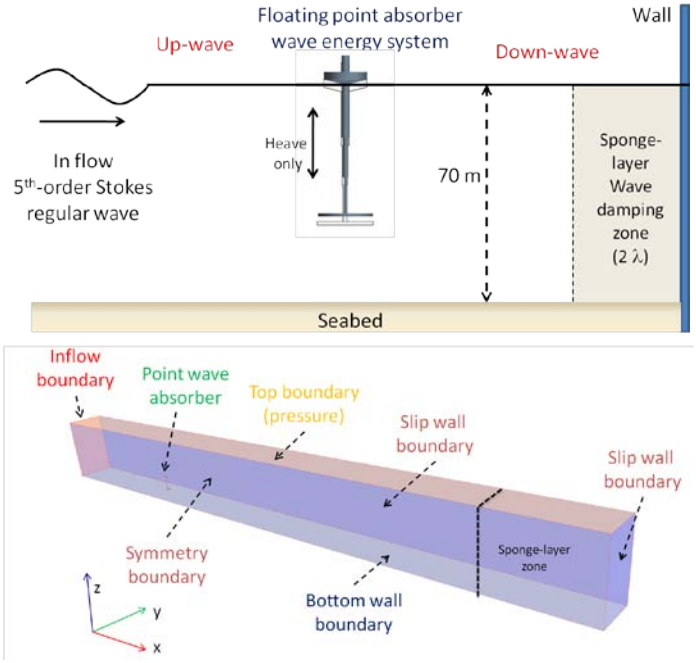

Figure 2. Computational domain and domain boundaries

FPA model and PTO

The geometry of the FPA was designed using SolidWorks. The designed weight of the full-scale model was about 249.5 metric tons, and the center of gravity was located 22.4 m below the mean free surface. The FPA geometry was further modified in the numerical model. The supporting jacket on the bottom of the central column and the detail of the reaction plate were further simplified. Nevertheless, the center of buoyancy was kept close to the SolidWorks design. Here, we only considered a basic structural design of the FPA model and ignored the effects of mooring lines.

As shown in Fig. 3, two FPA models were used in the study. The single body system assumes that the absorber was locked, and the whole device moved as a rigid body. All the parts were, therefore, moving in tandem. The two-body model assumed that the whole FPA model was separated into two sections, a floating one and a fully submerged one (neutrally buoyant), and the two were connected through the use of a mass-spring-damper system. The diameter of the vertical column sections was also modified to maintain the same immersed volume. Note that the investigation was not focused on the optimal control strategy or the feasible value of the spring stiffness. The spring was utilized only to connect the two sections, and a small value of 19.7 kN/m was applied. A damper was utilized to represent the PTO mechanism. F_{PTO} and the generated power P_{PTO} are defined as

$$F_{PTO} = C_{PTO} u_{FPA} \text{ and } P_{PTO} = C_{PTO} u_{FPA}^2, \quad (3)$$

where C_{PTO} is the damping coefficient, and u_{FPA} is the relative translating velocity between the floating section and the reaction section. The value of the damping coefficients used in most of the simulations was 254 kNsm^{-1}, which was on the same order of the one used in Agamloh et al. (2008) after scaling.

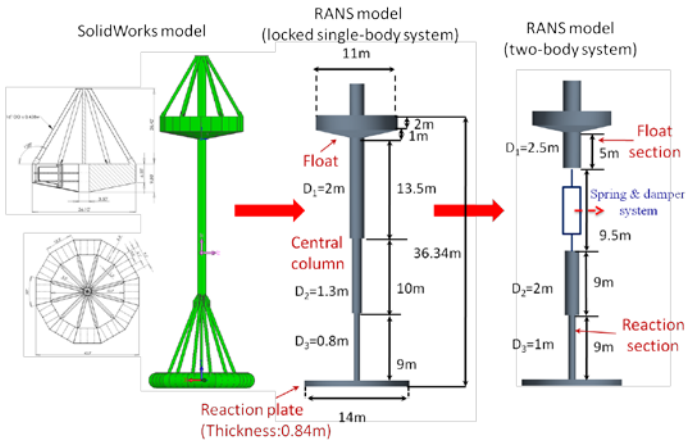

Figure 3. FPA geometry and dimensions

Meshing

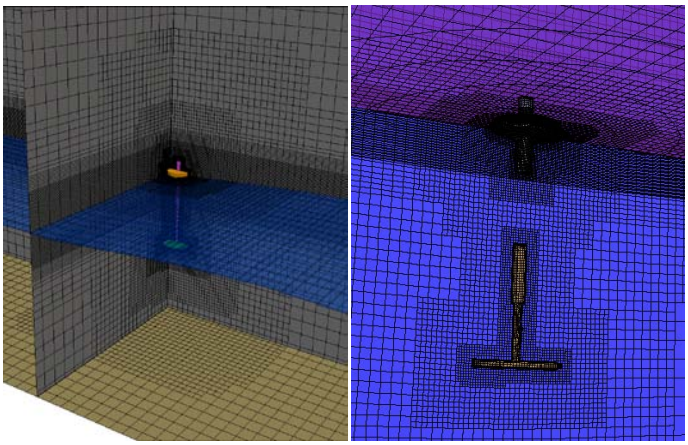

Figure 4. Mesh around the point wave absorber model

To capture both the wave dynamics and the details of the flow around the FPA, the mesh was finer near the free surface and near the FPA (Fig. 4), where hanging node cells also were implemented. In addition, prism-layer cells were placed along the FPA surface, and the height of the first layer was set so that the value of $y+$ satisfied the turbulence model requirement. Furthermore, the grid size Δx (in the wave propagation direction) was determined by the incident wavelength, and it was smaller than $\lambda/80$. The grid size Δz (in the vertical direction) near the free surface was adjusted according to the wave height H, and it was in the range between H/16 and H/24. The total number of cells for the mesh used in the RANS simulation was on the order of 0.8~1.0 million. Moreover, mesh morphing can create highly distorted cells if the time step is not sufficiently small. Therefore, a small time step of T/300 was utilized in the study, where T is the incident wave period. All the RANS simulations are carried out on NREL's high-performance computing (HPC) system[1]. It takes about 12 hours on 64 cores to complete 8~10 wave periods of time (approximately 3000 time steps).

VALIDATION

To validate the numerical prediction, a wave tank test was conducted at UC Berkeley's wave tank in December 2010. A 1:100 scale single body model was built based on the full scale SolidWorks design. When the FPA model was at rest, the mean water level was approximately 0.018m (model scale) from the top of the float, and wave tank was 68 m long, 2.4 m wide, and 1.5 m deep (Fig. 5).

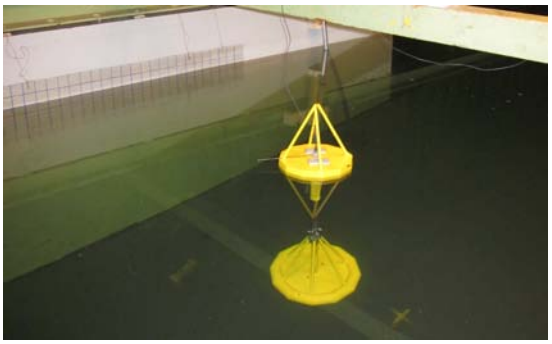

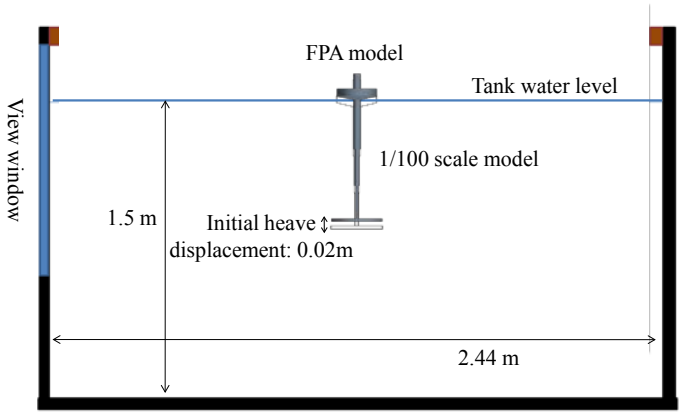

Figure 5. The single body FPA model in the experimental wave tank including tank dimensions

To capture the FPA motion, a 2D motion tracking system next to the wave tank was utilized, and the motion tracking system used passive markers on the buoy to create targets for the motion tracking software.

[1] Each compute node consists of dual socket/quad-core 2.93 GHz Intel Nehalem processor, with 12 GB of memory shared by all 8 cores.

The motions were captured as a 2D projection orthogonal in the direction of the propagation of waves in the tank. A LabVIEW data acquisition system, based on a National Instruments Compact RIO controller, with a channel-to-channel optically isolated analog input module (NI 9239), was used to collect the data.

The heave decay test was performed with an initial displacement of 0.02m (model scale). The comparison of the heave decay test between the RANS simulation and the experimental measurement is presented in Fig. 6. The heave decay period was about 10 seconds, and the RANS result agreed fairly well with the experimental data. A small discrepancy was probably due to the slight difference in the model geometry.

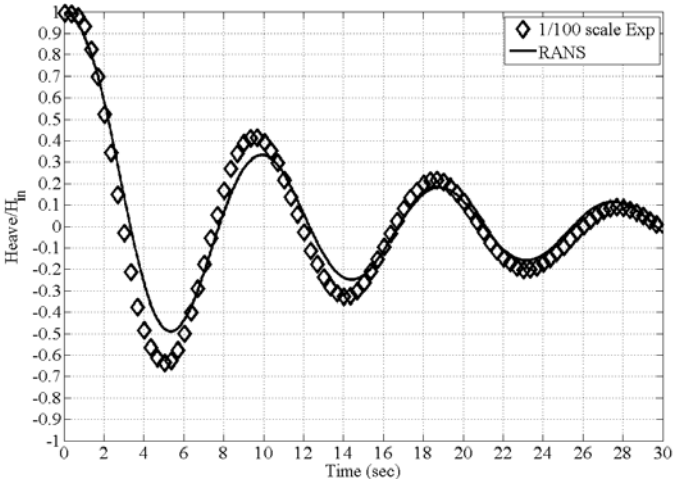

Figure 6. Heave decay from RANS and from the experimental measurement

REGULAR WAVES ANALYSIS

Both the single model and the two-body model were examined in the numerical wave tank through the use of the RANS method. A 5th-order Stokes wave was specified at the inflow boundary.

Single body FPA model

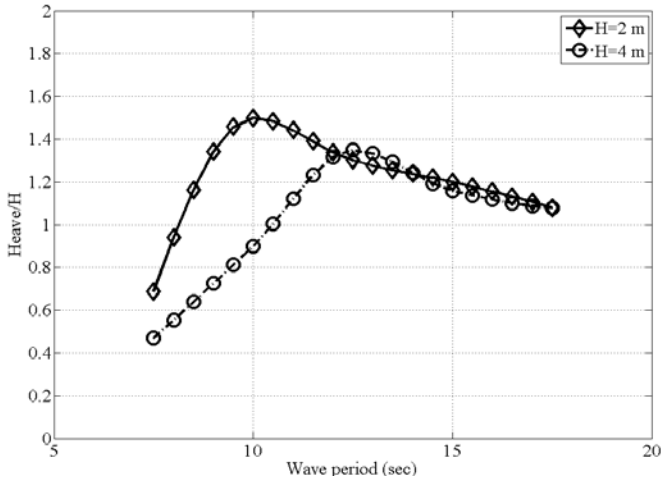

Figure 7. Comparison of the FPA response in heave (scaled by H) in 2 m and in 4 m waves

The heave response amplitude operator (RAO) of the (locked) single-body FPA model in two different incident wave heights, 2 m and 4 m; is plotted in Fig. 7. The heave response was proportional to the incident wave height for large wave period scenarios. A resonant period of 10 seconds was observed in the 2 m wave scenarios. This was consistent with the natural decay period obtained from the decay test. However, this resonance was not observed in the 4 m wave scenarios, and it is discussed in a later section.

The instantaneous heave response of the FPA in 2 m waves, with different wave periods and the linear theory-based wave elevation, are plotted in Fig. 8. When the wave period was large, the heave response generally followed the wave motion. On the other hand, the phase shift between the FPA heave motion and the wave elevation increased as the wave period became smaller. When the phase shift was increased, the nonlinear interaction between waves and the FPA model became more significant, especially under waves with larger wave heights.

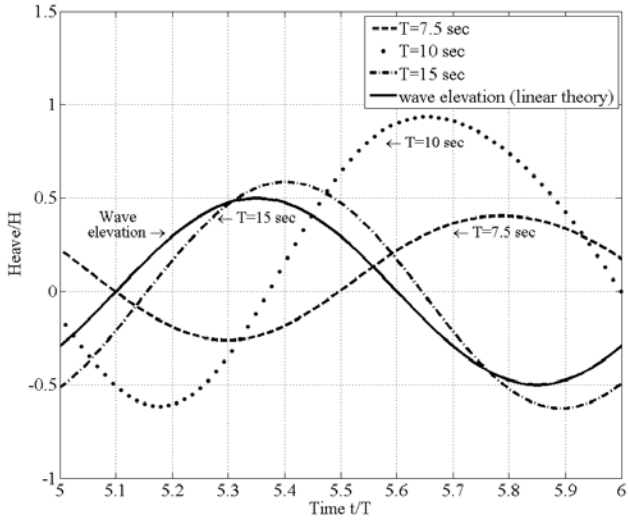

Figure 8. Heave response of the FPA model in waves

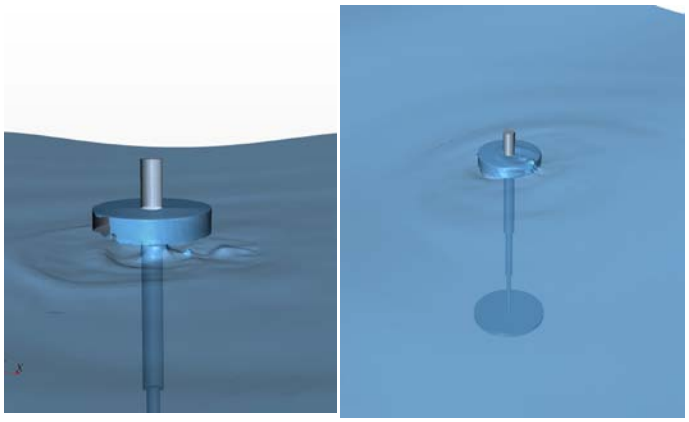

Figure 9. FPA model in waves at t/T=8.76 (left) and t/T=9.43 (right)

For this particular single body FPA model, wave overtopping was not observed in the 2 m wave scenarios. On the other hand, wave overtopping occurred in the FPA in the 4 m wave scenarios, when the wave period was smaller than 12 seconds. In one of the 4 m wave scenarios (T=7.5 seconds), the entire float was out of the water when t/T=8.76, and waves overtopped the float when t/T=9.43 (Fig. 9). This

suggests that wave overtopping could induce additional constraint on the FPA heave motion, as shown in Fig. 7, where the RAO for the 4 m wave scenarios was smaller than that for the 2 m wave scenarios when the wave period was smaller than 12.5 seconds.

Figure 10 shows the hydrodynamic pressure distribution near the FPA model at a time instant of t/T=9.43. Since the motion of fluid particles decreases rapidly with increasing depth below the free surface, the hydrodynamic wave impact on the float was more significant than on the reaction plate. Moreover, when wave overtopping occurred, the nonlinear hydrodynamic effect provided an additional damping force to reduce the FPA heave motion.

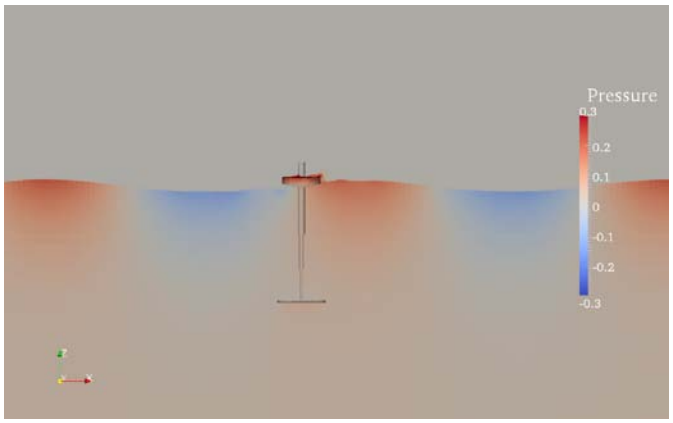

Figure 10. Hydrodynamic pressure (scaled by ρgD) contour around the single body FPA model (T=7.5seconds; H=4m)

Two-body FPA MODEL

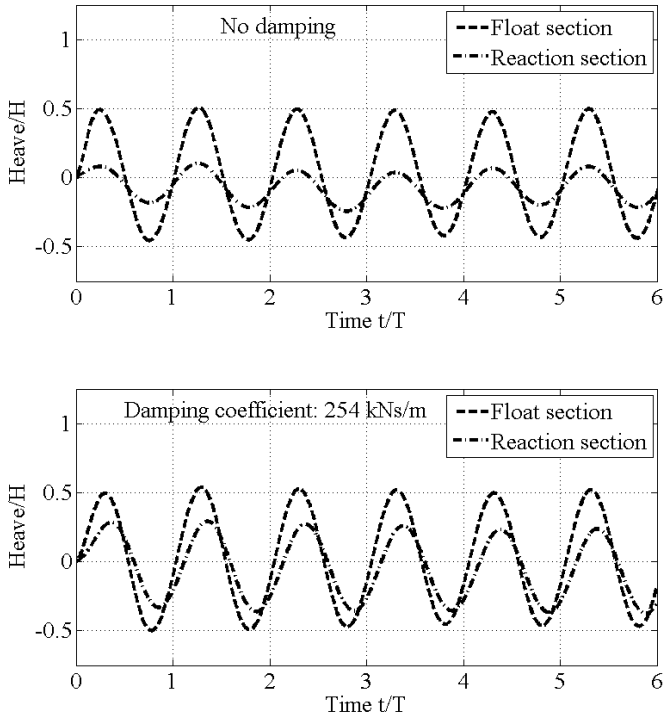

Figure 11. Heave response of the float and the reaction sections

This section presents the prediction for the hydrodynamic heave response of the two-body FPA model and an estimation of generated power, without applying any control method. The effect of PTO on the hydrodynamic response of the float and reaction sections was investigated here, where a wave with a height of 4 m and a period of 12.5 seconds was given. The heave response of the two sections, with and without the presence of PTO, is plotted in Fig. 11. Since the hydrodynamic wave effect decreases with the depth, the amplitude of the heave motion for the float section was greater than that for the reaction section. When PTO was considered, the relative motion between the two bodies was reduced, and a phase shift was induced.

An example of the instantaneous velocity of the two sections and the relative velocity u_{FPA} is plotted in Fig. 12. The generated power was calculated by following Eq. (3). It is proportional to the square of the relative translational velocity of the two sections.

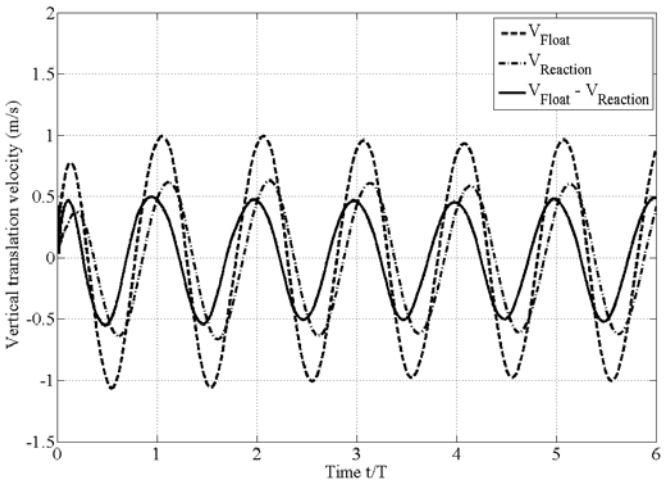

Figure 12. Translational velocities of the float and the reaction sections and the relative velocity between the two

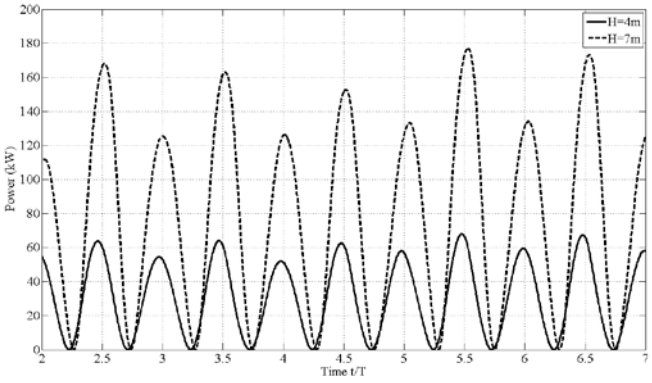

Figure 13. Instantaneous power of the two-body FPA system in waves (T=12.5 seconds)

The power generation under different wave heights also was investigated, and an example of the instantaneous power of the FPA system (with a given spring stiffness and a damping coefficient) is shown in Fig. 13. Through a series of RANS simulations (Fig. 14), the study showed that the generated power increased nonlinearly with the incident wave height. According to linear theory, the maximum wave absorption is proportional to H^2. However, the prediction from the

RANS method was less than that, especially when the wave period was smaller, and the nonlinear effects were more significant. This indicated that those nonlinear effects, created by the complex geometry of the two-body FPA, the mass-spring-damper system, the flow viscosity, and the nonlinear interaction between waves and the FPA, influenced the FPA motion as well as the resulting power generation in operational wave conditions.

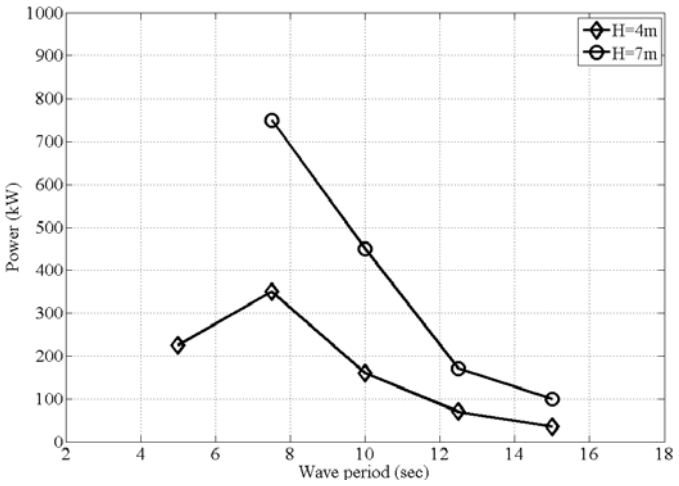

Figure 14. Maximum peak power generation for the two-body FPA system in different wave conditions (wave breaking occurred in the 7 m wave scenarios, when the wave period was smaller than 6 seconds)

In fact, wave overtopping was also observed in the large wave height scenarios. Figure 15 shows the hydrodynamic pressure contour around FPA along the z=0 plane at a time instant of t/T=5.38, where the wave height was 7 m and the wave period was 7.5 seconds. Similar to those single body FPA scenarios, the hydrodynamic pressure on the float section was increased and an additional heave reduction force was induced.

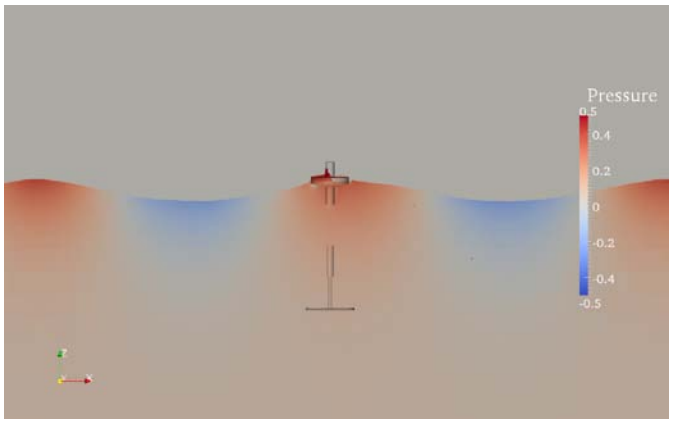

Figure 15. Hydrodynamic pressure (scaled by $\rho g D$) contour around the two-body FPA model (T=7.5seconds; H=7m)

According to Budal and Falnes (1975), the maximum wave power P_{max} that a heaving axisymmetric body can absorb is

$$P_{max} = JL_{max}, \tag{4}$$

where J is the wave energy flux, and L_{max} is the absorption width, which is defined as $L_{max}=\lambda/2\pi$. For linear deep-water waves, $\lambda=g/2\pi$ and $J=\rho g^2TH^2/(32\pi)$. Budal and Falnes (1980) proposed another upper limit (also referred to as Budal's upper bound) for the wave power P_u that can be absorbed by a given submerged body volume $\forall$. It is

$$\frac{P_u}{\forall} < \frac{\pi\rho gH}{4T}. \tag{5}$$

The two curves represent the theoretical prediction of the maximum wave energy that can be captured by a semi-submerged heaving body with optimum heaving amplitude (Falnes, 2007).

Figure 16 plots the RANS prediction of the maximum peak power generated from the heave motion of the two-body FPA and the comparison with the theoretical upper limit obtained from Eqs. (4) and (5). The point of intersection of the two theoretical curves can be defined as (T, P) = (T_c, P_c), where

$$T_c = (32\pi^4 g^{-2}\forall/H)^{1/4} \text{ and } P_c = (\rho g^{3/2}/8)(\forall^3 H^5/2)^{1/4}. \tag{6}$$

For this particular two-body FPA system, the resonance occurred when the incident wave period was around 7 seconds. In addition, given that no specific control method was applied in the RANS simulation, the power capturing efficiency was lower than the theoretical solution, as expected.

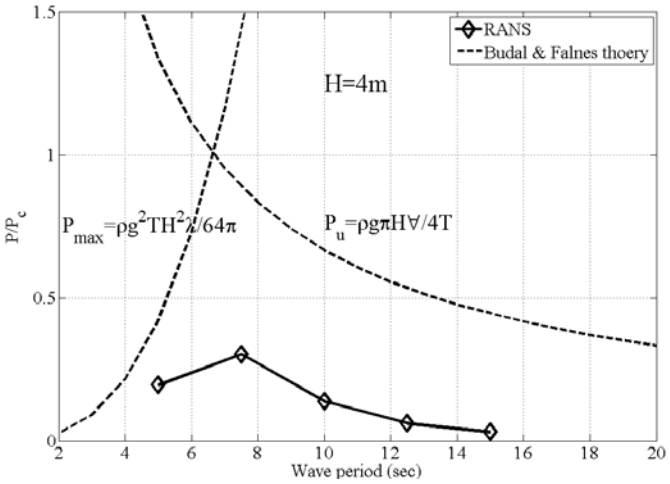

Figure 16. Maximum peak power generation for the FPA system from the RANS method and the theoretical curves for the maximum power absorption (modified after Falnes 2007)

DISCUSSION

The RANS simulation showed that the phase shift between the FPA heaving motion and the wave elevation increases as the wave period decreases. As a result, the nonlinear interaction between waves and the FPA device can be significant, and wave overtopping may occur. Given that the weight of the float section for the two-body FPA is less than the

weight of the single body FPA, the resonant period for the float section is smaller. Therefore, wave overtopping only was observed in the large wave scenarios. Nevertheless, the nonlinear effects can mitigate the FPA heave motion, and the resulting power output can be reduced.

For the maximum power generation analysis, Falnes (2007) mentioned that there is a significant improvement on the power absorption efficiency if latching control is applied. Furthermore, when control is applied and $T=T_c$, the maximum power absorption can reach up to 50% of the intersection value P_c, depending on the wave height, the immersed volume (buoyancy force), and the absorber geometry. However, our RANS simulation was performed with a constant value mass-spring-damper system, and the system was not optimal (no control was applied). As a result, the maximum power absorption was only about 30% of P_c, and the power absorption efficiency decreased rapidly in the sup-resonant period region. The application of control in the FPA system and the optimal geometry and dimension for the device requires further investigation.

CONCLUSIONS

This paper presented preliminary results of the hydrodynamics of a particular FPA obtained with a RANS model. The RANS model was first validated with the experiment in a heave decay test. Through a series of RANS simulations, the FPA heave response in waves was studied, with and without the present of PTO mechanism. In addition, the maximum power that the FPA can generate under operational wave conditions, with a constant value mass-spring-damper system, was also investigated. The study showed that the effect of the nonlinear interaction between waves and the FPA device on power generation can be significant, even in operational wave conditions, since power generation was directly associated with the motion of FPA. In addition, the maximum power absorption efficiency of this particular two-body FPA system was about 30% when the incident wave was at the resonant period. Overall, the performance of the FPA wave energy system is promising.

FUTURE WORK

There are a number of problems to be addressed in studying this particular FPA. The following summarizes intended future research:

- This RANS model is only validated with a single body decay test. More experimental tests, especially two-body tests, will be conducted for validation.
- The power prediction of the FPA's motion is without optimal control. Thus, a study on optimizing the power absorption efficiency, in both regular and irregular waves, is required. This will include the application of a control method and the feasible value of the damping coefficient for representing the PTO mechanism.
- Studies on the effects of the mooring system and other translational and rotational motions on power absorption efficiency are needed.
- More importantly, this study only focuses on the hydrodynamics of the FPA. A comprehensive design of an FPA should combine both hydrodynamics and power electronics as presented by Yeung et al. (2010) . Thus, a coupling study of this two-body FPA will be conducted.

REFERENCES

Agamloh, E., Wallace, A. and Von Jouanne, A. (2008). "Application of fluid-structure interaction simulation of an ocean wave energy extraction device", *Renewable Energy*, Vol. 33, No. 4, pp. 748-757.

Bjarte-Larsson, T. and Falnes, J. (2006). "Laboratory experiment on heaving body with hydraulic power take-off and latching control", *Ocean Engineering*, Vol. 33, No. 7, pp. 847-877.

Budal, K. and Falnes, J. (1975). "A resonant point absorber of ocean-wave power", *Nature*, Vol. 256, pp. 478-479, corrigendum 257:626.

Budal, K. and Falnes, J. (1980). "Interacting point absorbers with controlled motion", *Power from sea waves*, pp. 381-399.

Drew, B., Plummer, A. and Sahinkaya, M. (2009). "A review of wave energy converter technology", *Proceedings of the Institution of Mechanical Engineers, Part A: Journal of Power and Energy*, Vol. 223, No. 8, pp. 887-902.

Evans, D. (1976). "A theory for wave-power absorption by oscillating bodies", *Journal of Fluid Mechanics*, Vol. 77, No. 01, pp. 1-25.

Falcão, A. (2010). "Wave energy utilization: A review of the technologies", *Renewable and Sustainable Energy Reviews*, Vol. 14, pp. 899-918.

Falnes, J. (2002). "Ocean waves and oscillating systems", Cambridge University Press.

Falnes, J. (2007). "A review of wave-energy extraction", *Marine Structures*, Vol. 20, No. 4, pp. 185-201.

Korde, U. (1999). "Efficient primary energy conversion in irregular waves", *Ocean Engineering*, Vol. 26, No. 7, pp. 625-651.

Mei, C.C. (1976). "Power extraction from water waves", *Journal of Ship Research*, Vol. 20, pp. 63-66.

Thorpe, T.W. (1999). "A brief review of wave energy", Harwell Laboratory, Energy Technology Support Unit.

Yavuz, H., Stallard, T., McCabe, A. and Aggidis, G. (2007). "Time series analysis-based adaptive tuning techniques for a heaving wave energy converter in irregular seas", *Proceedings of the Institution of Mechanical Engineers, Part A: Journal of Power and Energy*, Vol. 221, No. 1, pp. 77-90.

Yeung, R.W., Peiffer, A., Tom, N. and Matlak, T. (2010). "Design, analysis,and evaluation of the UC-Berkeley wave-energy extractor", *Proc. 29th Int. Conf. on Ocean, Offshore and Arctic Eng.*, OMAE, Shanghai,China.

REPORT DOCUMENTATION PAGE

Form Approved
OMB No. 0704-0188

PLEASE DO NOT RETURN YOUR FORM TO THE ABOVE ORGANIZATION.

1. REPORT DATE *(DD-MM-YYYY)*	2. REPORT TYPE	3. DATES COVERED *(From - To)*
March 2011	Conference Paper	

4. TITLE AND SUBTITLE
A RANS Simulation of the Heave Response of a Two-Body Floating Point Wave Absorber: Preprint

5a. CONTRACT NUMBER
DE-AC36-08GO28308

5b. GRANT NUMBER

5c. PROGRAM ELEMENT NUMBER

6. AUTHOR(S)
Y. Yu and Y. Li

5d. PROJECT NUMBER
NREL/CP-5000-50980

5e. TASK NUMBER
WA10.7010

5f. WORK UNIT NUMBER

7. PERFORMING ORGANIZATION NAME(S) AND ADDRESS(ES)
National Renewable Energy Laboratory
1617 Cole Blvd.
Golden, CO 80401-3393

8. PERFORMING ORGANIZATION REPORT NUMBER
NREL/CP-5000-50980

9. SPONSORING/MONITORING AGENCY NAME(S) AND ADDRESS(ES)

10. SPONSOR/MONITOR'S ACRONYM(S)
NREL

11. SPONSORING/MONITORING AGENCY REPORT NUMBER

12. DISTRIBUTION AVAILABILITY STATEMENT
National Technical Information Service
U.S. Department of Commerce
5285 Port Royal Road
Springfield, VA 22161

13. SUPPLEMENTARY NOTES

14. ABSTRACT *(Maximum 200 Words)*
A preliminary study on a two-body floating wave absorbers is presented in this paper. A Reynolds-Averaged Navier-Stokes computational method is applied for analyzing the hydrodynamic heave response of the absorber in operational wave conditions. The two-body floating wave absorber contains a float section and a submerged reaction section. For validation purposes, our model is first assumed to be locked. The two sections are forced to move together with each other. The locked single body model is used in a heave decay test, where the RANS result is validated with the experimental measurement. For the two-body floating point absorber simulation, the two sections are connected through a mass-spring-damper system, which is applied to simulate the power take-off mechanism under design wave conditions. Overall, the details of the flow around the absorber and its nonlinear interaction with waves are investigated, and the power absorption efficiency of the two-body floating wave absorber in waves with a constant value spring-damper system is examined.

15. SUBJECT TERMS
RANS simulation; offshore wind turbines; two-body floating point wave absorber; Wave Energy Conversion (WEC); heave; Reynolds-averaged Navier-Stokes (RANS) equation; Volume Of Fluid (VOF); free surface; Floating-Point Absorber (FPA);Power Take Off (PTO)

16. SECURITY CLASSIFICATION OF:			17. LIMITATION OF ABSTRACT	18. NUMBER OF PAGES	19a. NAME OF RESPONSIBLE PERSON
a. REPORT	b. ABSTRACT	c. THIS PAGE			
Unclassified	Unclassified	Unclassified	UL		19b. TELEPHONE NUMBER (*Include area code*)